APPLICATION OF A SIMPLIFIED MODEL FOR ANALYSING AIRFLOW INTERACTION WITH BODIES OF VARIOUS SHAPES

Vitalijs Beresnevich[1], Janis Viba[1], Maris Eiduks[1], Martins Irbe[1], Edgars Kovals[1], Shravan Koundinya Vutukuru[2]
[1]Riga Technical University, Latvia;
[2]Vel Tech Rangarajan Dr Sagunthalla R and D Institute of Science and Technology, India
vitalijs.beresnevics@rtu.lv, janis.viba@rtu.lv, maris.eiduks@rtu.lv, martins.irbe@rtu.lv, edgars.kovals@gmail.com, vshravankoundinya1989@gmail.com

Abstract. Interaction between solid bodies and airflow is widely encountered in mechanical engineering and transportation systems. These interactions are commonly analyzed using computational fluid dynamics (CFD), which accounts for vortex formation and flow separation. However, such methods are primarily applied to stationary objects under steady-flow conditions and require significant computational resources. Therefore, there is a need for simplified analytical approaches applicable to both stationary and moving bodies. This paper presents a simplified analytical model for airflow-body interaction based on a two-dimensional representation of the object as a cylindrical prism. The approach assumes steady flow conditions and introduces a constant coefficient to describe suction-side interaction. The interaction forces are derived using a differential-integral formulation based on classical fluid mechanics, resulting in a system of ordinary differential equations. Analytical relationships are obtained for bodies with different geometries, including cylindrical and segment-type profiles. A parametric analysis shows that the drag-related coefficient varies nonlinearly with geometric parameters, exhibiting both a local minimum and a maximum within the investigated range. For example, the horizontal force coefficient ranges from approximately 1.37 to 2.20 depending on the configuration. In addition, the model predicts negative lift at small angles of attack, which is consistent with known aerodynamic behaviour. The proposed method enables efficient estimation of interaction forces and supports shape optimization and motion analysis without the need for full CFD simulations. The novelty of the work lies in the development of a unified analytical framework that reduces the problem to ordinary differential equations while retaining the essential features of airflow interaction.

Keywords: airflow-body interaction, modelling, aerodynamic forces, shape optimization, prism geometry.

Introduction

The mechanical motion of objects is governed by the laws of physics that describe their interactions with the surrounding environment and other bodies [1-3]. In the analysis of interactions between solid objects and fluids (air or water), two empirical coefficients are widely used: the drag coefficient (C_d) and the lift coefficient (C_l) (e.g., [4]). The values of these coefficients differ for three-dimensional and two-dimensional models and experiments, and they also depend on whether the motion is steady or unsteady (e.g. [5; 6]).

Numerous experimental, theoretical, and computational studies have therefore been conducted. These studies enable comparison of results and support further calculations in the analysis of object motion. For example, studies [7-10] investigate the interaction of viscous fluid flow with plates of a given length, as well as the influence of gusts and the aerodynamic behaviour of flat square objects. In experimental research, most investigations have been carried out under steady-flow conditions with stationary objects in standard wind tunnels [11-15]. Similar studies of horizontal flow motion in a rectangular overflow well are presented in [16]. To obtain a more accurate assessment of the redistribution of fluid interactions in the frontal and rear regions of objects, experimental and modelling studies have been conducted to investigate suction effects [17-19]. Extensive experimental and computational investigations have also been performed to provide a more complete description of the drag coefficient for fluid interactions with objects of relatively simple shapes, such as plates and cylinders [20-24].

Owing to fundamental research in fluid dynamics, it is now possible to perform analytical calculations for moving objects in a moving fluid environment [25-29]. However, most existing approaches either rely on computationally intensive numerical methods or provide analytical descriptions limited to simplified geometries or stationary conditions. As a result, there remains a lack of unified analytical models capable of describing airflow interaction with bodies of various shapes under both stationary and moving conditions. The aim of the present study is to develop a simplified analytical approach for modelling airflow-body interaction that enables the derivation of tractable analytical relationships for engineering analysis and optimization.

The novelty of the proposed approach lies in representing the interaction as a combination of frontal and suction components and reducing the governing equations to a system of ordinary differential equations with variable coefficients. This enables efficient analysis of interaction forces and motion characteristics without the need for full-scale CFD simulations.

Models and methods of analysis

The interaction between a fluid and a solid object strongly depends on the initial conditions of motion and on the spatial constraints surrounding the object under consideration. In many cases, these interaction processes are simplified by assuming either that the object is stationary while the fluid moves around it, or conversely, that the fluid is stationary while the object moves through it.

In the present study, the following assumptions are adopted: the flow is considered steady; the interaction is analyzed within a two-dimensional framework; viscous and turbulent effects are taken into account in an approximate manner through empirical coefficients; and the object geometry is represented by simplified analytical shapes. Under these assumptions, the interaction forces can be described using reduced-order analytical models. Previous studies (e.g. [26; 29]) indicate that such assumptions are acceptable, as the results can be verified experimentally or numerically. Therefore, this approach is also adopted in the present study. In addition, the developed methodology allows an approximate analysis of the motion of objects in a moving fluid environment.

Interaction of a stationary sectoral prism with flow

A model of the interaction between a stationary sectoral prism and airflow is shown in Fig. 1.

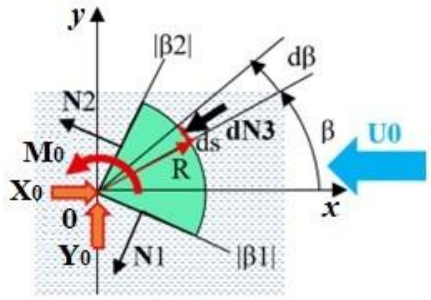

Fig. 1. **Interaction of a stationary sectoral prism with airflow:** $x0y$ – fixed coordinate system; U_0– air-flow velocity parallel to the x axis; R – sector radius; β – orientation angle of the frontal elementary interaction surface; $d\beta$ – elementary angular increment; ds – length of the elementary arc; dN_3 – elementary surface reaction; N_1, N_2 –suction forces acting on the plane sides; X_O, Y_O, and M_O – force and moment components of the reactions at point 0 of the fixed prism

In the proposed model, it is assumed that the frontal interaction of the flow occurs on the curved surface of the prism, whereas the two flat surfaces are subjected to suction effects. The orientation of these surfaces is determined by the sector boundary angles β_1 and β_2. The reaction forces acting on the plane surfaces in the normal directions, $N_1$and N_2, as well as the local interaction force acting on the frontal surface, dN_3, are determined as follows [25; 26]:

$$N_1 = C\rho RBU_0^2 \cdot (\cos\beta_1)^2 ; N_2 = C\rho RBU_0^2 \cdot (\cos\beta_2)^2; dN_3 = \rho \cdot ds \cdot BU_0^2 \cdot (\cos(d\beta))^2; \quad (1)$$

$$ds = R \cdot d\beta, \quad (2)$$

where C – dimensionless empirical coefficient accounting for suction-side interaction;
ρ – fluid density, kg·m^{-3};
R – sector radius, m;
B – prism height, m;
ds – elementary arc length of interaction, m;
$d\beta$ – elementary increment of the angle β, rad.

The coefficient C used in the mathematical model depends on the geometry of the rear surface and the flow conditions and is typically determined from experimental data or calibrated using numerical

simulations. According to experimental results reported in [26], the value $C = 0.065$ was obtained in a wind tunnel for a perforated plate. In the present study, the value $C = 0.1$ is adopted as a representative approximation that accounts for geometric differences.

In the case of prism equilibrium, the reactions at the fixing point 0 can be determined from the following equations:

$$X_0 - N_1 \cdot \cos\beta_1 - N_2 \cdot \cos\beta_2 - \rho R B U_0^2 \cdot \int_{\beta 1}^{\beta 2} (\cos\beta)^3 \cdot \mathrm{d}\beta \; = \; 0\,, \tag{3}$$

$$Y_0 - N_1 \cdot \sin\beta_1 \; + \; N_2 \cdot \sin\beta_2 - \rho R B U_0^2 \cdot \int_{\beta 1}^{\beta 2} (\cos\beta)^2 \cdot \sin\beta \cdot \mathrm{d}\beta \; = \; 0\,, \tag{4}$$

$$M_0 - N_1 \cdot \frac{R}{2} \; + \; N_2 \cdot \frac{R}{2} \; = \; 0\,, \tag{5}$$

where X_0 and Y_0 – the reaction forces caused by the interaction forces, N;
X_0 – the reaction moment caused by the interaction, N·m.

The obtained expressions (3)-(5) can be used in static analysis and optimisation problems solving, as well as in dynamic studies by substituting these relations into the corresponding differential equations.

Optimization of the interaction of a two-plane truncated cylinder

The cylinder of the considered shape has two slits (Fig. 2). One slit is located along the diameter, while the other is oriented at an angle γ to the flow direction. Similarly to the previous analysis described by equations (1)-(5), integration leads to the following expressions:

$$X_0 \; = \; \rho R B U_0^2 \cdot \left\{ 2(\sin\gamma)^4 \; + \; 2C \; + \; \left[\frac{3(\cos\gamma)^2}{2} - \frac{(\cos 3\gamma)^2}{6} \right] \right\}, \tag{6}$$

$$Y_0 \; = \; \rho R B U_0^2 \cdot \left\{ (\sin\gamma)^3 \cdot \cos\gamma \; + \; 0 \; + \; \left[\frac{\sin(2\gamma)}{4} - \frac{\sin(6\gamma}{12} \right] \right\}, \tag{7}$$

$$M_0 = 0. \tag{8}$$

The obtained expressions (6) and (7) can be used for shape optimisation when determining the minimum or maximum values of the forces X_0 and Y_0 as functions of the parameter γ. For example, to determine the extreme values of the horizontal interaction force, the following expression for the coefficient $DF_x(\gamma)$ can be analysed:

$$DF_x(\gamma) \; = \; \frac{X_0}{\rho R B U_0^2} \; = \; \left\{ 2(\sin\gamma)^4 \; + \; 2C \; + \; \left[\frac{3(\cos\gamma)^2}{2} - \frac{(\cos 3\gamma)^2}{6} \right] \right\}, \tag{9}$$

The graph of the function $DF_x(\gamma)$ is shown in Fig. 3 for $C = 0.1$.

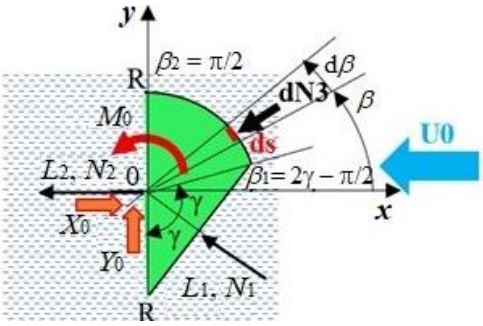

Fig. 2. **Model of a two-plane truncated cylinder:** L_1, L_2 – plane edges; γ – sector half-angle as an optimization parameter

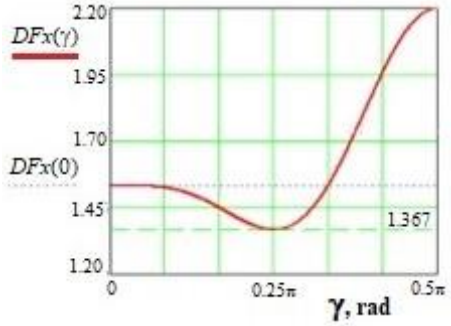

Fig. 3. **Variation of the horizontal force coefficient DF_x as a function of the sector half-angle γ, illustrating the nonlinear dependence and the presence of local extrema**

The obtained graph shows that this function has a local maximum at $\gamma = 0$, a minimum at $\gamma = 0.25\ \pi$, and a supremum at $\gamma = 0.50\ \pi$ within the interval $0 \leq \gamma \leq 0.50\ \pi$. Values of the coefficient DF_x at some characteristic points of the graph are as follows: $DF_x(0) = 1.533$; $DF_x(0.25\pi) = 1.367$; $DF_x(0.5\pi) = 2.20$. Additionally, the analysis of the graph (Fig. 3) reveals another effect: in the pressure zone, the force decreases within a certain range when a cylindrical surface is replaced by a flat surface.

Interaction of the sides of a segmental slice pyramid

The model of a possible wing configuration to be analysed consists of one flat surface and one cylindrical surface (Fig. 4). The objective of the analysis is to determine the interaction forces as functions of the flow angle of attack α. Similarly to the previous analysis, the following relations are obtained for the range $0 < \alpha < \gamma$:

$$X_0 = \rho R B U_0^2 \cdot \{\left[\int_{\frac{\pi}{2}-\gamma}^{\frac{\pi}{2}-\alpha} \left(\sin\left(\frac{\pi}{2} + \alpha - \beta\right)\right)^2 \cdot \sin\left(\frac{\pi}{2} + \alpha - \beta\right) \cdot d\beta\right] +$$

$$+(-C) \cdot \left[\int_{\frac{\pi}{2}-\alpha}^{\frac{\pi}{2}+\gamma} \left(\sin\left(\frac{\pi}{2} + \alpha - \beta\right)\right)^2 \cdot \sin\left(\frac{\pi}{2} + \alpha - \beta\right) \cdot d\beta\right] + (-2) \cdot (\sin\alpha)^2 \cdot \cos\alpha \cdot \sin\gamma\}, \quad (10)$$

$$Y_0 = \rho R B U_0^2 \cdot \{\left[\int_{\frac{\pi}{2}-\gamma}^{\frac{\pi}{2}-\alpha} \left(\sin\left(\frac{\pi}{2} + \alpha - \beta\right)\right)^2 \cdot \cos\left(\frac{\pi}{2} + \alpha - \beta\right) \cdot d\beta\right] +$$

$$+(-C) \cdot \left[\int_{\frac{\pi}{2}-\alpha}^{\frac{\pi}{2}+\gamma} \left(\sin\left(\frac{\pi}{2} + \alpha - \beta\right)\right)^2 \cdot \cos\left(\frac{\pi}{2} + \alpha - \beta\right) \cdot d\beta\right] + (-2) \cdot (\sin\alpha)^2 \cdot \sin\alpha \cdot \sin\gamma\}, \quad (11)$$

$$M_0 = 0. \quad (12)$$

where α – angle of attack, rad;
γ – half-angle of the segment centre, rad;
β – variable integration angle (Fig. 4), rad.

As in the previous case, expressions (10) and (11) can be used to solve analysis and optimisation problems. For example, after integration of expression (11), relation (13) is obtained for analysing the vertical reaction force Y_0 in the following form:

$$Dy(\alpha) = \frac{Y_0}{\rho R B U_0^2} = \frac{(\sin 2\alpha)^3}{3} - \frac{(\sin(\gamma + \alpha))^3}{3} + C \cdot \left(\frac{(\sin 2\alpha)^3}{3} - \frac{(\sin(\alpha - \gamma))^3}{3}\right) + 2\sin\gamma \cdot \cos\alpha \cdot (\sin\alpha)^2. \quad (13)$$

An example of the graph of the function $Dy(\alpha)$ for a central angle of $2\ \gamma = 0.5\ \pi$ (rad) and for $C = 0.1$ is shown in Fig. 5. Extremal values of the coefficient *Dy* obtained at some characteristic points of the graph are as follows: Dy (0.122) = –0.129; Dy (0.785) = 0.533.

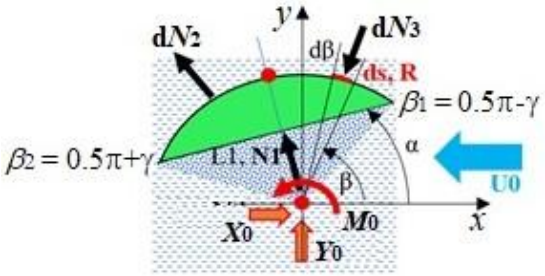

Fig. 4. **Model of a segmental slice pyramid: dN_2, dN_3 – elementary interaction forces acting on the curved surfaces of the segment**

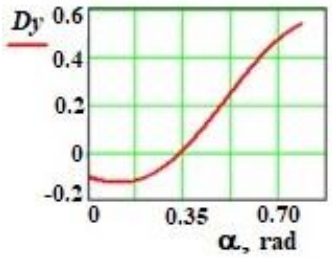

Fig. 5. **Dependence of the lift-related coefficient Dy on the angle of attack α, demonstrating the variation of aerodynamic response (for $0 < \alpha < \gamma$)**

From the graph shown in Fig. 5, it follows that at small angles of attack ($0 \leq \alpha < 0.35$ rad) the lift force is negative ($Dy < 0$). This result is well known in aerodynamics (see, for example, [30]). Furthermore, it should be noted that the commonly cited explanation that a "longer path" in the upstream region of an airfoil necessarily produces positive lift is not always valid.

Analysis of the flight dynamics of a sports javelin

The flight dynamics model of a sports javelin is shown in Fig. 6. The sharp ends and elongated shape of the javelin can be approximately described by a segmental cut if the excess surface at the boundary approaches a plane. Using procedures like those previously applied in determining air resistance, the following equations of motion in the stationary reference frame $x0y$ can be obtained:

$$m\ddot{x} = -N\sin\varphi; \tag{14}$$

$$m\ddot{y} = N\cos\varphi; \tag{15}$$

$$J_c\ddot{\varphi} = M_A - Nd. \tag{16}$$

The normal component N of the flow interaction forces and the moment of air interaction M_A at the reduction centre A are described by the following equations:

$$N = (1 + C)\rho B\int_{-\frac{L}{2}}^{\frac{L}{2}}(-\dot{x}\sin\varphi + y\dot{c}os\varphi - \xi\dot{\varphi})^2\cdot\varepsilon d\xi\,, \tag{17}$$

$$NM_A = (1 + C)\rho B\int_{-\frac{L}{2}}^{\frac{L}{2}}(-\dot{x}\sin\varphi + \dot{y}\cos\varphi - \xi\dot{\varphi})^2\cdot\varepsilon\cdot\xi d\xi\,, \tag{18}$$

where ε – can take the value ± 1 and is defined as $\varepsilon = \text{sign}(-\dot{x}\sin\varphi + \dot{y}\cos\varphi - \xi\dot{\varphi})$.

Other notations used in the model are as follows:

φ – angular coordinate of the javelin during rotational motion, rad;
ξ– variable distance of the javelin section from the reduction center A, m;
m, J_c – mass of the javelin (kg) and its moment of inertia about the centre of mass C (kg·m^2);
ρ – medium density, kg·m^{-3};
d, h – coordinates of the center of mass relative to the reduction point A, m;
L, B – length and width of the javelin, m.

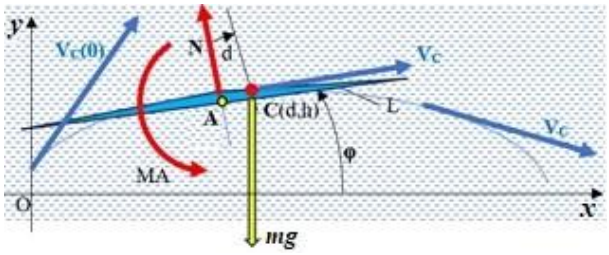

Fig. 6. **Schematic representation of the planar motion model of a sports javelin, showing the centre of mass *C*, the point *A* of resultant aerodynamic force application (at the midpoint of the javelin), and the velocity vector V_C**

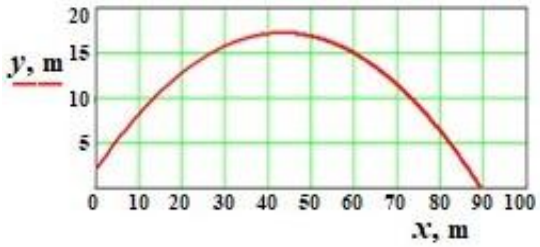

Fig. 7. **Motion trajectory of the centre of mass of the javelin in the *x*0*y* plane**

The results of a numerical modelling example are shown in Fig. 7-9 for the following parameters:

ρ = 1.25 kg·m^{-3}; m = 1 kg; C = 0.1; B = 0.05 m; L = 1 m; $J_c = m\ L^2\cdot 12^{-1}$; g = 9.81 m·s^{-2}; d = 0.01 m; $x(0)$ = 0 m; $y(0)$ = 2 m; $\varphi(0)$ = 0.611 rad; $\dot{x}(0) = 30\cos\varphi(0)$ m·s^{-1}; $\dot{y}(0) = 30\cdot\sin\varphi(0)$ m·s^{-1}; $\dot{\varphi}(0)$ = -0.25·s^{-1}.

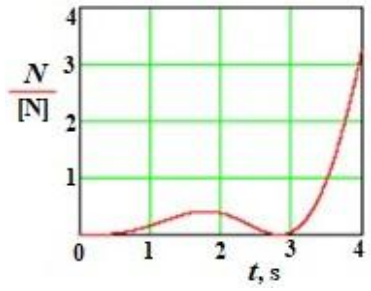

Fig. 8. **Normal component *N* of the interaction force as a function of time *t* during the motion**

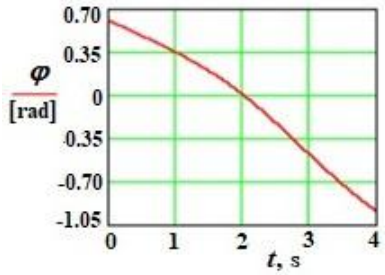

Fig. 9. **Rotation angle *φ* as a function of time *t* during the motion process**

The resulting graphs indicate that the initial conditions can be varied within a certain range to obtain the maximum flight distance when the javelin reaches the ground.

Results and discussion

Analytical studies conducted on flat and cylindrical objects confirm that continuous interaction forces with the surrounding environment can be approximately described by analyzing the frontal and suction sides of the object separately. In this approach, ordinary differential equations with variable parameters can be used instead of partial differential equations.

In the analysis of the planar flight motion of a javelin, the interaction is considered by decomposing the motion into translational and rotational components. As a result, the main problem is reduced to evaluating surface integrals over the object surface with a variable projection of the flow velocity onto the surface normal. In addition, the interaction on the suction side must also be considered, and its influence is described by the coefficient *C*, which requires experimental determination.

The validity of the proposed analytical approach is supported by previous studies [26], in which a comparison with experimental data for a plate oscillating in an unsteady airflow showed a discrepancy within 10-12%. Furthermore, CFD simulations for bodies of rhombic shape reported in [26] also demonstrated good agreement with the analytical model under steady-flow conditions. These results suggest that the proposed approach can provide reasonable estimates of interaction forces for engineering applications within the considered assumptions. At the same time, it should be noted that the present study does not include direct experimental or numerical validation for the specific geometries and motion conditions considered. Therefore, further investigations involving dedicated experiments and CFD simulations are required to extend the validation of the model.

Overall, the results demonstrate that the proposed simplified analytical approach provides a practical and computationally efficient tool for estimating interaction forces and analysing the motion of bodies with relatively simple geometric shapes.

Conclusions

1. The results of the present study indicate that, within the adopted assumptions of steady two-dimensional flow and simplified geometry, the interaction between airflow and a solid body can be described using a reduced-order analytical framework formulated as a system of ordinary differential equations. This formulation may serve as a practical tool for approximate analysis and preliminary optimization of mechanical systems without direct reliance on CFD methods.
2. The proposed approach suggests that the interaction forces can be approximated by separately considering the frontal and suction regions of the body surface. However, the accuracy of this representation depends on the empirical coefficient *C*, which reflects the characteristics of the suction-side interaction and requires further refinement based on experimental or numerical data.
3. The present model should be regarded as an approximate and condition-dependent analytical framework. Its applicability to real aerodynamic configurations requires further validation against experimental measurements or high-fidelity numerical simulations. Future work will focus on extending the approach to more complex geometries and combined translational-rotational motion, as well as on systematic validation of the model.

Author contributions

Conceptualization, J.V. and S.K.V.; methodology, V.B. and E.K.; software, J.V. and M.E.; validation, M.I. and V.B.; formal analysis, E.K., S.K.V. and M.E.; investigation, M.I., V.B., J.V. and E.K.; data curation, V.B.; writing – original draft preparation, V.B.; writing – review and editing, J.V. and V.B.; visualization, J.V. and M.E.; project administration, V.B. All authors have read and agreed to the published version of the manuscript.

References

[1] Newton I. The Mathematical Principles of Natural Philosophy. Newtons Principia. Translated into English by Andrew Motte. Princeton: Princeton University, 1846. 594 p.
[2] Christodoulou D. The Euler equations of compressible fluid flow. Bulletin (New Series) of the American Mathematical Society, vol. 44, No. 4, 2007, pp. 581-602.
[3] Bennett A. Lagrangian Fluid Dynamics. Cambridge: Cambridge University Press, 2006. 286 p.
[4] Hoerner S.F. Fluid – Dynamic Drag. Publisher: Liselotte A. Hoerner, USA, 1965. 455 p.
[5] Jeremy V. Turbulent flow and drag over fixed two- and three-dimensional dunes. Journal of Geophysical Research Atmospheres, vol. 112(F4), 2007, pp. 1-21. DOI: 10.1029/2006JF000650
[6] Jourdan G., Igra O., Estivalèzes J-L. Drag coefficient of a sphere in a non-stationary flow: New results. Proceedings of the Royal Society A, 463(2088), 2007, pp. 3323-3345. DOI: 10.1098/rspa.2007.0058
[7] Balashov A.A., Dudin G.N. Investigation of flow past a flat plate in the strong interaction regime. Fluid Dynamics, vol. 53, 2018, pp. 394-401. DOI: 10.1134/S0015462818030035
[8] Afgan I., Benhamadouche S., Han X., Sagaut P., Laurence D. Flow over a flat plate with uniform and coherent gust inlets. Journal of Fluid Mechanics, vol. 720, 2013, pp. 457-485. DOI: 10.1017/jfm.2013.25
[9] An H., Cheng L., Zhao M. Direct numerical simulation of oscillatory flow around a circular cylinder at low Keulegan-Carpenter number. Journal of Fluid Mechanics, vol. 666, 2011, pp. 77-103. DOI: 10.1017/S0022112010003691
[10] Chern M.-J., Lu Y.-J., Chang S.-C., Cheng I.-C. Interaction of oscillatory flows with a square cylinder. Journal of Mechanics, vol. 23(04), 2007, pp. 445-450.
[11] Wang H., Lu C., Qu C., Xiong J. Experimental investigation on flow field around a flapping plate with single degree of freedom. Nuclear Engineering and Technology, vol. 55, issue 6, 2023, pp. 1999-2010. DOI: 10.1016/j.net.2023.02.030
[12] Sopan Rahtika I.P.G., Wardana I.N.G., Sonief A.A., Siswanto E. Experimental investigation on flutter similitude of thin-flat plates. Advances in Acoustics and Vibration, article ID 7091425, 2017, pp. 1-8. DOI: 10.1155/2017/7091425
[13] Ozgoren M., Okbaz A., Dogan S., Sahin B., Akilli H. Investigation of flow characteristics around a sphere placed in a boundary layer over a flat plate. Experimental Thermal and Fluid Science, vol. 44, 2013, pp. 62-74. DOI: 10.1016/j.expthermflusci.2012.05.014
[14] Liao B., Chen S. Experimental study of flow past obstacles by PIV. Procedia Engineering, vol. 126, 2015, pp. 537-541. DOI: 10.1016/j.proeng.2015.11.300
[15] Xu Y.-Z., Feng L.-H., Wang J-J. Experimental investigation on the flow over normal flat plates with various corner shapes. Journal of Turbulence, vol. 16(7), 2015, pp. 607-616. DOI: 10.1080/14685248.2015.1018421
[16] Bhajantri M.R., Eldho T.I., Deolalikar P.B. Hydrodynamic modelling of flow over a spillway using a two-dimensional finite volume-based numerical model. Sadhana, vol. 31(6), 2006, pp. 743-754. DOI: 10.1007/BF02716893
[17] Thummar M., Bhoraniya R., Narayanan V. Effects of non-uniform suction and injection on the flat-plate boundary layer characteristics. Fluid Mechanics and Fluid Power, vol. 2, 2023, pp.25-30. DOI: 10.1007/978-981-19-6970-6_5
[18] Joshi K., Soto C., Bhattacharya S. Hydrodynamics of a twisting flat plate: experiments and inviscid modelling using leading-edge-suction parameter. Journal of Fluid Mechanics, vol. 1017: A40, 2025, pp. 1-27. DOI: 10.1017/jfm.2025.10495

[19] Corelli Grappadelli M., Asaro S., Radespiel R., Badrya C. Experimental investigations on boundary layer transition over a flat plate with suction and comparison with linear stability theory. Experiments in Fluids, vol. 66, 154. 2025, pp. 1-20. DOI: 10.1007/s00348-025-04084-z
[20] Theis A., Voll L., Diehl K., Heymsfield A., Giammanco I., Borrmann S., Szakáll M. A wind tunnel investigation into the aerodynamics of natural hailstones. Journal of the Atmospheric Sciences, online publication, 2025. DOI: 10.1175/JAS-D-25-0015.1
[21] Souza P.V.S., Girardi D., de Oliveira P.M.C. Drag force in wind tunnels: A new method. Physica A: Statistical Mechanics and its Applications, vol. 467, 2017, pp. 120-128. DOI: 10.1016/j.physa.2016.09.049
[22] Rasuo B. Scaling between wind tunnels – results accuracy in two-dimensional testing. Transactions of the Japan Society for Aeronautical and Space Sciences, vol. 55(2), 2012, pp. 109-115. DOI: 10.2322/tjsass.55.109
[23] Sanwar A. Sunny. Study of the wind tunnel effect on the drag coefficient (CD) of a scaled static vehicle model compared to a full scale computational fluid dynamic model. Asian Journal of Scientific Research, vol. 4(3), 2011, pp. 236-245. DOI: 10.3923/ajsr.2011.236.245
[24] Awbi H.B., Tan S.H. Effect of wind-tunnel walls on the drag of a sphere. Journal of Fluids Engineering, vol. 103(3), 1981, pp. 461-465. DOI: 10.1115/1.3240816
[25] Viba J., Beresnevich V., Irbe M. Synthesis and optimization of wind energy conversion devices. In: Design Optimization of Wind Energy Conversion Systems with Applications; Editor K. Maalawi. London: IntechOpen, 2020, pp. 125–141. DOI: 10.5772/intechopen.90819
[26] Viba J., Beresnevich V., Irbe M. Methods and Devices for Wind Energy Conversion. In: Wind Turbines - Advances and Challenges in Design, Manufacture and Operation; Editor K. Maalawi. London: IntechOpen, 2022, pp. 247-270. DOI: 10.5772/intechopen.103120
[27] Viba J., Beresnevich V., Noskovs S., Irbe M. Investigations of rotating blade for energy extraction from fluid flow. Vibroengineering Procedia, vol. 8, 2016, pp. 312-315. [online] [16.06.2026] Available at: https://www.extrica.com/article/17676
[28] Viba J., Beresnevich V., Irbe M., Dobelis J. The control of blades orientation to air flow in wind energetic device. Energy Procedia, vol. 128, 2017, pp. 302-308. DOI: 10.1016/j.egypro.2017.08.317
[29] Viba J., Tipans I., Irbe M., Vutukuru S.K. Optimization of energy extraction using definite geometry prisms in airflow. Latvian Journal of Physics and Technical Sciences, vol. 58(2), 2021, pp. 19-31. DOI: 10.2478/lpts-2021-0009
[30] Czyz Z., Karpinski P., Ruchata P., Matijošius J. Evaluation of the influence of the support on the aerodynamic characteristics of the tested object. Advances in Science and Technology Research Journal, vol. 20(1), 2026, pp. 30-47. DOI: 10.12913/22998624/208412